

HKRAG: Holistic Knowledge Retrieval-Augmented Generation Over Visually-Rich Documents

Anyang Tong^{1*} Xiang Niu^{1*} Zhiping Liu¹ Chang Tian² Yanyan Wei¹ Zenglin Shi^{1†} Meng Wang¹
¹Hefei University of Technology ²KU Leuven

Abstract

Existing multimodal Retrieval-Augmented Generation (RAG) methods for visually rich documents (VRD) are often biased towards retrieving salient knowledge (e.g., prominent text and visual elements), while largely neglecting the critical fine-print knowledge (e.g., small text, contextual details). This limitation leads to incomplete retrieval and compromises the generator’s ability to produce accurate and comprehensive answers. To bridge this gap, we propose HKRAG, a new holistic RAG framework designed to explicitly capture and integrate both knowledge types. Our framework features two key components: (1) a Hybrid Masking-based Holistic Retriever that employs explicit masking strategies to separately model salient and fine-print knowledge, ensuring a query-relevant holistic information retrieval; and (2) an Uncertainty-guided Agentic Generator that dynamically assesses the uncertainty of initial answers and actively decides how to integrate the two distinct knowledge streams for optimal response generation. Extensive experiments on open-domain visual question answering benchmarks show that HKRAG consistently outperforms existing methods in both zero-shot and supervised settings, demonstrating the critical importance of holistic knowledge retrieval for VRD understanding.

1. Introduction

Retrieval-augmented generation (RAG) has emerged as a leading paradigm to enhance the factual accuracy of large language models (LLMs) by grounding them in external knowledge sources [5, 7, 31]. Traditionally, RAG frameworks operate under the assumption of a purely textual corpus. However, a vast amount of real-world information is encapsulated within visually rich documents (VRDs), such as reports, invoices, and web pages, where meaning is conveyed through an intricate interplay of textual and visual elements (e.g., layout, typography, images) [14, 20, 28, 29,

*These authors contributed equally.

†Corresponding author: zenglin.shi@hfut.edu.cn

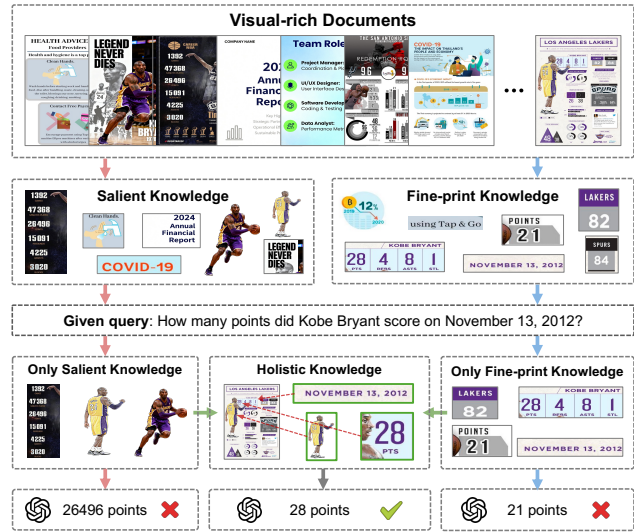


Figure 1. We demonstrate that both salient knowledge and fine-print knowledge are critical for retrieval and generation. Only by jointly leveraging both can we produce reliable answers and effectively mitigate hallucinations.

32]. Applying text-centric RAG to these multimodal documents creates a significant modality gap, leading to substantial information loss and unreliable generation.

Recognizing this limitation, several studies [8, 19, 39] have explored multimodal RAG for document visual question answering (DocumentVQA), typically leveraging large vision-language models (LVLMs) [5, 31]. These methods aim to establish a query-to-document alignment by projecting both queries and document images into a shared embedding space. While a step forward, their retrieval mechanism remains fundamentally biased. They are primarily adept at capturing salient knowledge, *i.e.*, information that is visually prominent through large fonts, central placement, or high contrast. Consequently, they often fail to retrieve fine-print knowledge: critical details embedded in small text, footnotes, or dense contextual passages. This bias results in incomplete retrieval, and when the retrieved, saliency-

biased context is passed to an LVLM, the generator lacks the necessary context to produce fully accurate answers, especially for queries hinging on nuanced details.

We argue that a comprehensive understanding of VRDs demands holistic knowledge, which necessitates the integration of both salient and fine-print knowledge. The former provides the global context and main points, while the latter contains essential qualifications, conditions, and precise details. However, achieving this is profoundly challenging for two reasons. First, from a retrieval perspective, simultaneously identifying sparse fine-print elements and broad salient features within a complex document is difficult, as standard similarity search tends to be dominated by salient signals. Second, in generation, simply concatenating all retrieved information is suboptimal; the generator must dynamically assess which pieces of knowledge—salient or fine-print—are most relevant to the query and integrate them coherently.

To address these challenges, we propose HKRAG, a novel RAG framework designed for holistic knowledge retrieval and generation over VRDs. Our approach consists of two key components. First, we introduce a *Hybrid Masking-based Holistic Retriever*. It employs explicit masking approaches to separately model and enhance the embeddings for salient and fine-print content within a document, ensuring a query-relevant retrieval process that captures both knowledge types. Second, we develop an *Uncertainty-guided Agentic Generator*. This module does not passively process all retrieved documents. Instead, it first dynamically selects a minimal sufficient set of documents. Then, based on the uncertainty of the initial answers, it adaptively decides how to fuse the complementary information from the salient and fine-print knowledge sources to arrive at a final, well-grounded response.

To summarize, our contributions are as follows:

- We identify and formalize a critical limitation in existing multimodal RAG methods for VRDs: their bias towards salient knowledge and their failure to retrieve fine-print knowledge, which leads to the *inadequate holistic knowledge problem*.
- We propose the HKRAG framework, which features (1) a novel hybrid masking-based retriever for balanced knowledge retrieval and (2) an uncertainty-aware agentic generator for dynamic knowledge integration.
- Extensive experiments on open-domain DocumentVQA benchmarks demonstrate that HKRAG consistently outperforms the existing methods in both zero-shot and supervised settings, validating its effectiveness and generalizability.

2. Related work

Retrieval-augmented generation. RAG aims to construct and retrieve external knowledge bases to reduce the genera-

tion of hallucinatory content and enhance model credibility across diverse tasks [5–7, 9, 31]. Traditional RAG methods have achieved remarkable success in natural language processing tasks and have been effectively extended to diverse domains such as images, videos, and audio [18, 26]. However, most approaches tend to originate from an academic research perspective, relying on knowledge retrieval from clean corpora [2, 23, 37]. In this paper, we focus on retrieving visually rich documents from real-world open-domain scenarios, where answers can only be derived from the documents [14, 20, 28, 29, 32]. Additionally, the content within these documents is presented in diverse formats, encompassing both prominent and nuanced knowledge that often requires integration to correctly respond to queries. Consequently, establishing an effective RAG pipeline for these documents remains a challenge.

RAG for document visual question answering. Visual documents are widely used in real-life scenarios and present content in diverse formats [14, 20, 29]. To retrieve query-relevant knowledge from visual documents, traditional RAG methods [11, 15, 16, 27, 33, 34] typically rely on text detection techniques (OCR) to scan textual information within documents, severely neglecting the vast amount of visual information present. Visual large language models (LVLMs) [5, 31, 36], which combine visual encoders with large language models, have gained widespread attention for their image understanding capabilities. Existing RAG methods, *e.g.*, VisRAG [39], DSE [19], ColPali [8], and VDocRAG [30] for visual documents employ LVLM encoding for both queries and documents, constructing image-based knowledge bases and retrieving knowledge by calculating similarity between external knowledge and queries [8, 19, 30, 39]. These methods classically leverage query-document alignment to enhance retrieval performance. However, we pinpoint that simultaneously identifying sparse fine-print elements and broad salient features within a complex document is difficult, as standard similarity search tends to be dominated by salient signals. Second, in generation, simply concatenating all retrieved information is suboptimal; the generator must dynamically assess which pieces of knowledge—salient or fine-print—are most relevant to the query and integrate them coherently.

3. Method

3.1. Problem Formulation

In the open-domain document visual question answering (DocumentVQA) task, the retriever \mathcal{R} filters query-relevant documents from external visually rich document set and supplies them to the generator \mathcal{G} to improve answer reliability. Both \mathcal{R} and \mathcal{G} are built upon a large vision-language model (LVLM) with a dual-encoder architecture, encoding queries and documents independently. Specifi-

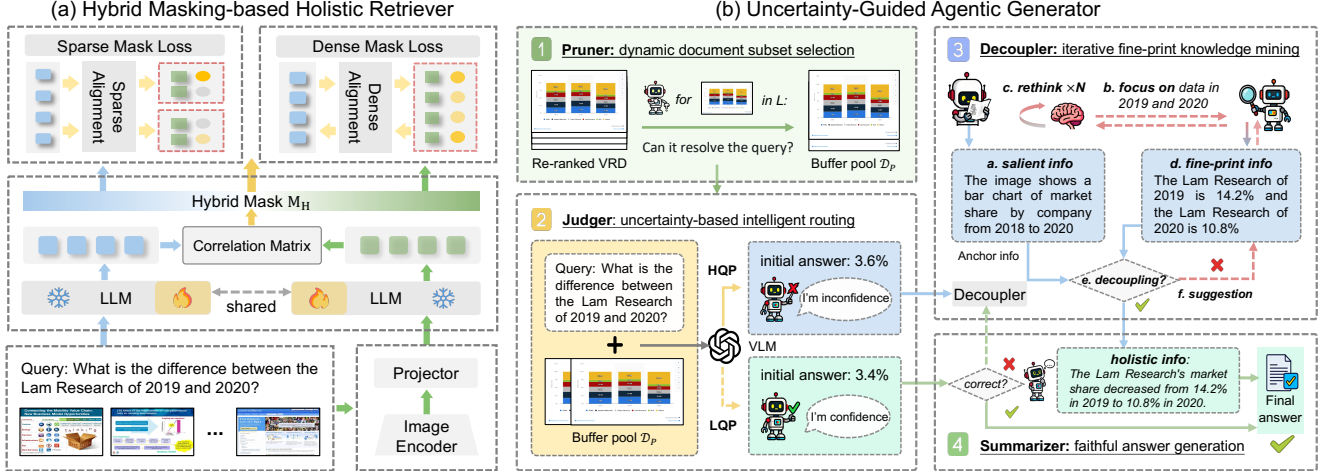


Figure 2. The proposed HKRAG includes (a) Hybrid Masking-based Holistic Retriever and (b) Uncertainty-Guided Agentic Generator.

cally, given a textual query q and a collection of N visual documents represented as images $\mathcal{D} = \{d_1, d_2, \dots, d_N\}$, the retriever is defined as a function $\mathcal{R} : (q, \mathcal{D}) \rightarrow \mathcal{D}_{\mathcal{R}}$, which takes q and \mathcal{D} as inputs, and returns a ranked subset $\mathcal{D}_{\mathcal{R}} = \{d_{r_1}, d_{r_2}, \dots, d_{r_k}\} \subset \mathcal{D}$ based on a search algorithm. $\mathcal{D}_{\mathcal{R}}$ often consists of the fixed top- k documents most relevant to q . For the query q and retrieved results $\mathcal{D}_{\mathcal{R}}$, the generator can be defined as a function $\mathcal{G} : (q, \mathcal{D}_{\mathcal{R}}) \rightarrow a$, which takes q and $\mathcal{D}_{\mathcal{R}}$ as inputs and concatenates their features to feed into LLM for generating the answer a .

A fundamental limitation of existing multimodal RAG methods in this setting is their inherent bias towards salient knowledge. These methods lack the capability to recognize and retrieve fine-print knowledge. This results in a failure to capture the holistic knowledge necessary for comprehensive document understanding. Consequently, the generator often produces answers based on an incomplete context, leading to factual inaccuracies and hallucinations, especially for queries that require reasoning over subtle details. To overcome this limitation, we propose HKRAG, a framework designed to explicitly model and integrate both knowledge types. It introduces (1) a hybrid masking-based holistic retriever for balanced retrieval of salient and fine-print knowledge, and (2) an uncertainty-guided agentic generator for dynamic, iterative integration of the retrieved knowledge to produce faithful answers.

3.2. Hybrid Masking-based Holistic Retriever

To retrieve the query-relevant holistic knowledge from the document set, we first obtain the embeddings of queries and documents. Specifically, each document image undergoes scaling and dynamic cropping processes, which decomposes complex global information into simpler local ones. The resulting document image patches are processed by a

visual encoder and subsequently projected into document features through a two-layer MLP. Next, both the query and visual document features are fed into a LLM, from which we extract their final-layer embeddings (v_q, v_d) , where document embedding v_d carries substantial information and shares the same dimensions as query embedding v_q .

Hybrid embedding-masking. We then design a hybrid embedding-masking approach that contains a dense mask to localize salient knowledge within query-relevant documents, along with a sparse mask to pinpoint the fine-print knowledge. We begin by normalizing embeddings (v_q, v_d) to obtain v_q^n and v_d^n , then compute their correlation as $C_{q,d} = |v_q^n \odot v_d^n|$. To accommodate document features with varying visual information densities and ensure accurate masking, we further scale the correlation values to the range $(0, 1)$, defined by $C_{q,d}^n$:

$$C_{q,d}^n = \left(1 + \exp \left(-\frac{C_{q,d} - \mu_{C_{q,d}}}{\sigma_{C_{q,d}} + \epsilon} \right) \right)^{-1}, \quad (1)$$

where ϵ is a negligible value, $\mu_{C_{q,d}}$ and $\sigma_{C_{q,d}}$ denote the mean and variance of $C_{q,d}$, respectively. Notably, the mean $\mu_{C_{q,d}^n}$ and variance $\sigma_{C_{q,d}^n}$ represent the average level and the fluctuation degree of correlation $C_{q,d}^n$ between queries and documents, respectively. By adjusting their magnitudes, we define the correlation-based hybrid mask M_H as follows:

$$M_H = (\mathbb{1}(C_{q,d}^n > (\mu_{C_{q,d}^n} - \alpha \cdot \sigma_{C_{q,d}^n})) + \mathbb{1}(C_{q,d}^n > (\mu_{C_{q,d}^n} + \alpha \cdot \sigma_{C_{q,d}^n}))) / 2, \quad (2)$$

where α represents the hybrid scaling parameter. The hybrid mask leverages dense masking downward to preserve low-correlation detail features, thereby maintaining embedding diversity and avoiding dominant biases. Simultaneously, it employs sparse masking upward to amplify

highly correlated salient contexts, enhancing discernible focal points while suppressing irrelevant noise.

□ **Bidirectional retriever-tuning.** Our goal is not only to bridge the modality gap between textual queries and visual documents, but also to leverage the designed hybrid mask to effectively extract query-relevant holistic knowledge within rich visual documents. Specifically, we first employ InFoNCE [24] as a manner to bridge the modality gap. Positive pairs are formed from query-document pairs (q, d^+) , while in-batch negatives are used to compute the contrastive loss $\mathcal{L}_{\text{IN}}(v_q, v_{d^+})$ as follows:

$$\mathcal{L}_{\text{IN}}(v_q, v_{d^+}) = -\log \frac{\exp(\text{sim}(v_q, v_{d^+})/\tau)}{\sum_{i=1}^{\mathcal{B}} \exp(\text{sim}(v_q, v_{d_i})/\tau)}, \quad (3)$$

where $\text{sim}(\cdot, \cdot)$ denotes the cosine similarity function. τ is a temperature scaling parameter, and \mathcal{B} represents the batch size. To achieve more accurate query-to-document alignment, we employ the hybrid mask to compute the dense matching loss \mathcal{L}_{DIN} :

$$\mathcal{L}_{\text{DIN}} = \frac{1}{2}(\mathcal{L}_{\text{IN}}(v_q, v_{d^+} \cdot \mathbf{M}_H) + \mathcal{L}_{\text{IN}}(v_{d^+} \cdot \mathbf{M}_H, v_q)). \quad (4)$$

We enhance the alignment between queries and documents in the embedding space, which facilitates the extraction of salient knowledge. To further exploit fine-print knowledge, we utilize \mathcal{N} partial masks to compute the sparse matching loss \mathcal{L}_{SIN} as follows:

$$\mathcal{L}_{\text{SIN}} = \frac{1}{\mathcal{N}} \sum_{i=1}^{\mathcal{N}} \mathcal{L}_{\text{IN}}(v_q, v_{d^+} \cdot \mathbf{M}_H^i), \quad (5)$$

where \mathbf{M}_H^i and \mathbf{M}_H^{i+1} have the same dimensions, $\mathbf{M}_H^i \cap \mathbf{M}_H^{i+1} = 0$, and $\mathbf{M}_H = \bigcup_{i=1}^{\mathcal{N}} \mathbf{M}_H^i$. The mask partitioning positions are randomized to ensure alignment of details from diverse regions. We employ the loss $\mathcal{L} = \mathcal{L}_{\text{DIN}} + \beta \cdot \mathcal{L}_{\text{SIN}}$ to fine-tune the retriever, where β adjusts the contribution ratio between \mathcal{L}_{DIN} and \mathcal{L}_{SIN} . The retriever learns to map queries and relevant documents into closer proximity within the embedding space, effectively amplifying its sensitivity to query-relevant holistic knowledge.

3.3. Uncertainty-Guided Agentic Generator

Merely concatenating all retrieved information can overwhelm the generator and introduce noise. To enable a more intelligent integration of the retrieved holistic knowledge (encompassing both salient and fine-print knowledge), we introduce an uncertainty-based criterion to classify query-document pairs. Specifically, we define low-uncertainty query-document pair (LQP) and high-uncertainty query-document pair (HQP) below.

Definition 1 (Low-uncertainty Query-document Pair, LQP). *Given a query q and retrieved documents $\mathcal{D}_{\mathcal{R}}$, we feed them*

into LVLMM Θ to obtain an initial answer $\hat{a} = \Theta(q, \mathcal{D}_{\mathcal{R}})$ and its token sequence $\hat{w} = \{\hat{w}_1, \hat{w}_2, \dots, \hat{w}_L\}$. We further calculate the average entropy $\mathcal{H}(\hat{w}) = -\frac{1}{L} \sum_i^L (\hat{w}_i \cdot \log(\hat{w}_i))$ of \hat{w} and normalize it to obtain $\mathcal{H}'(\hat{w}) \in (0, 1)$. When $\mathcal{H}'(\hat{w})$ is lower than the uncertainty threshold h , we define this pair as a low-uncertainty query-document pair.

Definition 2 (High-uncertainty query-document pair, HQP). *Given a query q and retrieved documents $\mathcal{D}_{\mathcal{R}}$, we compute $\mathcal{H}'(\hat{w})$ according to Definition 1. When $\mathcal{H}'(\hat{w})$ is higher than the uncertainty threshold h at time t , we define this pair as a high-uncertainty query-document pair at time t .*

An LQP indicates that the LVLMM can derive sufficient query-relevant knowledge from the provided documents to produce a confident response, no need of further processing. In contrast, an HQP suggests that the initial understanding is inadequate, often due to the need to reconcile subtle relationships between salient and fine-print knowledge. For HQP, we introduce iterative, time-aware reasoning to facilitate deeper knowledge extraction via test-time computing. Building on this classification, we design an uncertainty-guided agentic generator composed of four specialized agents: *Pruner*, *Judger*, *Decoupler*, and *Summarizer*. The overall architecture and interaction flow of these agents are illustrated in Figure 2.

□ **Pruner: dynamic document subset selection.** Existing methods often employ fixed top- k document rankings empirically for generation. While higher k values increase the probability of retrieving query-relevant knowledge, they simultaneously introduce substantial irrelevant noise, particularly when processing visually rich documents, where abundant prominent information obscures query-relevant details. To address this issue, we introduce a pruner that evaluates total query-relevant knowledge $\mathcal{I}(q, n)$ of top- n retrieved documents based on LVLMM Θ , defined as

$$\mathcal{I}(q, n) := \sum_i^n \Theta(q, d_i), d_i \in \mathcal{D}_{\mathcal{P}} \quad (6)$$

where d_i is stored in a dynamic buffer pool $\mathcal{D}_{\mathcal{P}}$ with capacity k ($n < k$). When $\mathcal{I}(q, n)$ can answer the query q , the evaluation process terminates; otherwise, the buffer retains the top- k documents. Finally, $\mathcal{I}(q, n)$ is next passed to the *Judger*.

□ **Judger: uncertainty-based intelligent routing.** Beyond ensuring that sufficient knowledge $\mathcal{I}(q, n)$ is retrieved, assessing the reliability of the generated answer is more important. To address this, we introduce a *Judger* that evaluates whether the generator can confidently answer a given query. Specifically, the *Judger* categorizes each query-document pair according to Equations 1 and 2. Queries with low uncertainty are deemed straightforward and sent directly to the final agent, the Summarizer, for efficient processing. In contrast, queries with high uncertainty,

Datasets	Documents	#Images	#Train	#Test
ChartQA [20]	Chart	20,882	–	150
OpenWikiTable [14]	Table	1,257	4,261	–
SlideVQA \ddagger [29]	Slide	52,380	–	760
VisualMRC [28]	Webpage	10,229	6,126	–
InfoVQA [22]	Infographic	5,485	9,592	1,048
DocVQA [21]	Industry	12,767	6,382	–
DUDE [32]	Open	27,955	2,135	496
MHDocVQA \ddagger	Open	28,550	9,470	–

Table 1. We evaluate our models under both zero-shot and supervised settings. The *zero-shot* evaluation measures their ability to generalize to unseen datasets, whereas the *supervised* evaluation quantifies performance when training data is provided. \ddagger denotes datasets requiring multi-hop reasoning.

indicating a potential need to reconcile subtle relationships between salient and fine-print knowledge, are routed to the *Decoupler* for deeper analysis. Notably, the initial answer produced during uncertainty measurement is neither used as model input nor reflected upon, preventing historical outputs from biasing subsequent decisions.

□ Decoupler: iterative fine-print knowledge mining. We further introduce a *Decoupler* to deal with the high-entropy queries passed from the *Judger*. The query-relevant salient knowledge is denoted as $\mathcal{I}_h(q, n)$. This information often shares the semantic similarity with the query q but fails to accurately answer it. Therefore, we perform iterative, fine-grained reasoning to mine overlooked fine-print knowledge $\mathcal{I}_d(q, n, t)$ by anchoring on the readily available salient knowledge $\mathcal{I}_h(q, n)$ at time step t :

$$\mathcal{I}_d(q, n, t) = \Theta(\mathcal{I}_h(q, n), \mathcal{I}_d(q, n, t-1)). \quad (7)$$

To prevent the model from conflating two knowledge types and thereby stimulating the discovery of crucial details that are initially missed, we explicitly decouple them:

$$\mathcal{I}'_d(q, n, t) = \Theta(\mathcal{I}_h(q, n), \mathcal{I}_d(q, n, t)). \quad (8)$$

When the explored fine-print knowledge $\mathcal{I}'_d(q, n, t)$ can answer the query or reach the maximum iteration count; we feed both the decoupled salient information and detail information to the *Summarizer*.

□ Summarizer: faithful answer generation.

Finally, the *Summarizer* serves as the synthesis point for all information flows. It receives inputs from two paths: direct, low-uncertainty cases from the *Judger*, and comprehensively reasoned information from the *Decoupler*. For the former, it performs a final verification. For the latter, it refines and integrates the global context and fine details to generate the final, faithful answer. Through this structured collaboration, our agentic generator dynamically adapts its

reasoning depth, ensuring both efficient processing of simple queries and comprehensive understanding of complex ones.

4. Experiments

Data sources and settings. As the first collection of open-domain visually rich documents, OpenDocVQA integrates multiple DocumentVQA datasets that span a broad range of real-world document types, as summarized in Table 1. Following the protocol in [30], we evaluate model performance on these public datasets under both supervised and zero-shot settings. To more faithfully reflect real-world usage scenarios, we further conduct evaluations under two retrieval configurations: single-pool and all-pool. In the single-pool setting, retrieval is restricted to the document pool corresponding to each individual dataset. In contrast, the all-pool setting requires models to retrieve from a unified, large-scale corpus drawn from diverse domains, providing a more realistic and challenging assessment of retrieval robustness and cross-domain generalization.

Implementation details. For fair comparison, we initialize our retriever with Phi3V [1], a state-of-the-art LVLm trained on high-resolution and multi-image datasets, consistent with prior works [19, 30]. We fine-tune the retriever using LoRA [10] under two configurations—with and without pre-training, while keeping the generator settings identical to those in [30]. In HKRAG, the retriever and generator use independent parameter sets, and all other components remain frozen during fine-tuning. Training is conducted for one epoch using eight NVIDIA RTX 4090 GPUs, with the AdamW optimizer [17], FlashAttention [3] acceleration, and a batch size of 64. The temperature parameter τ is set to 0.01, submask number \mathcal{N} is set to 2, and the *Judger*’s uncertainty threshold is fixed at 0.8.

Unified evaluation metrics. We evaluate retrieval performance using the nDCG@5 metric, a widely adopted standard in information retrieval [8, 13]. For generation evaluation, we follow [35] and uniformly report accuracy. Specifically, we use the powerful Qwen-plus model to assess the quality of each prediction against its ground-truth answer, assigning a score on a 1–5 scale. A score of 4 indicates a generally correct but less concise response, while a score of 5 corresponds to a fully correct answer. Predictions receiving either score are treated as correct, and all others are counted as incorrect.

4.1. Retrieval Results

We evaluate HKRAG-Retriever against two categories of retrievers. The first category comprises off-the-shelf text retrieval models and image retrieval models, including BM25 [27], Contriver [11], E5 [33], GTE [16], E5-Mistral [34], NV-Embed-v2 [15], CLIP [25], DSE [19], and VisRAG-Ret

Model	Initialization	Docs	Scale	#PT	#FT	ChartQA		SlideVQA		InfoVQA		DUDE	
						Single	All	Single	All	Single	All	Single	All
<i>Off-the-shelf</i>													
BM25 [27]	–	Text	0	0	0	54.8	15.6	40.7	38.7	50.2	31.3	57.2	47.5
Contriever [11]	BERT [4]	Text	110M	1B	500K	66.9	59.3	50.8	46.5	42.5	21.0	40.6	29.7
E5 [33]	BERT [4]	Text	110M	270M	1M	74.9	66.3	53.6	49.6	49.2	26.9	45.0	38.9
GTE [16]	BERT [4]	Text	110M	788M	3M	72.8	64.7	55.4	49.1	51.3	32.5	42.4	36.0
E5-Mistral [34]	Mistral [12]	Text	7.1B	0	1.85M	72.3	70.0	63.8	57.6	60.3	33.9	52.2	45.2
NV-Embed-v2 [15]	Mistral [12]	Text	7.9B	0	2.46M	75.3	70.7	61.7	58.1	56.5	34.2	43.0	38.6
CLIP [25]	Scratch	Image	428M	400M	0	54.6	38.6	38.1	29.7	45.3	20.6	23.2	17.6
DSE [19]	Phi3V [1]	Image	4.2B	0	5.61M	72.7	68.5	73.0	67.2	67.4	49.6	55.5	47.7
VisRAG-Ret [39]	MiniCPM-V [38]	Image	3.4B	0	240K	87.2*	75.5*	74.3*	68.4*	71.9*	51.7*	56.4	44.5
<i>Trained on OpenDocVQA</i>													
Phi3 [1]	Phi3V [1]	Text	4B	0	41K	72.5	65.3	53.3	48.4	53.2*	33.0*	40.5*	32.0*
VDocRetriever † [30]	Phi3V [1]	Image	4.2B	0	41K	80.8	71.2	66.0	60.4	63.9*	48.3*	44.1*	35.6*
VDocRetriever † [30]	Phi3V [1]	Image	4.2B	500K	41K	84.4	76.3	75.3	69.9	70.4*	53.9*	55.6*	47.9*
HKRAG-Retriever	Phi3V [1]	Image	4.2B	0	41K	83.7	77.0	69.5	62.4	65.8*	52.1*	45.4*	40.6*
HKRAG-Retriever	Phi3V [1]	Image	4.2B	500K	41K	87.6	82.1	76.2	72.5	72.4*	57.8*	58.9*	51.7*

Table 2. Comparison of HKRAG’s retrieval performance against embedding-based models and existing approaches in both single-pool and all-pool settings across four open-domain DocumentVQA benchmarks. FT and PT indicate finetuning and pretraining, respectively. * indicates performance on test data for which corresponding training samples are available, and † denotes reproduced results.

Generator	Retriever	Docs	ChartQA		SlideVQA		InfoVQA		DUDE	
			Single	All	Single	All	Single	All	Single	All
Phi3 [1]	–	–	12.7	12.7	23.7	23.7	18.1*	18.1*	8.9*	8.9*
Phi3 [1]	Phi3 [1]	Text	17.7	17.5	32.4	32.1	21.0*	20.3*	15.4*	13.7*
VDocGenerator [30]	VDocRetriever [30]	Image	54.0	51.3	52.2	53.9	39.4*	36.2*	37.3*	36.9*
HKRAG-Generator	HKRAG-Retriever	Image	60.7	58.0	56.5	56.6	42.7*	39.6*	45.2*	42.7*
Phi3 [1]	Gold	Text	23.2	23.2	33.4	33.4	23.7*	23.7*	21.5*	21.5*
VDocGenerator [30]	Gold	Image	77.3	77.3	72.1	72.1	54.1*	54.1*	64.5*	64.5*
HKRAG-Generator	Gold	Image	78.7	78.7	74.0	74.0	54.7*	54.7*	68.8*	68.8*

Table 3. DocumentVQA results. All models are fine-tuned on OpenDocVQA. The results marked with * denote performance on unseen test samples, and the other results represent zero-shot performance. The performance gain in green is compared to the text-based RAG that has the same base LLM. Gold knows the ground-truth documents. Models answer the question based on the top three retrieval results.

[39]. The second category consists of models fine-tuned on the OpenDocVQA dataset.

Table 2 showcases the strong performance of HKRAG across four open-domain DocumentVQA benchmarks under both supervised and zero-shot settings. In the zero-shot setting on ChartQA and SlideVQA, HKRAG achieves new state-of-the-art results, with particularly notable gains in the challenging all-pool scenario (82.1% on ChartQA and 72.5% on SlideVQA). On the supervised benchmarks InfoVQA and DUDE, HKRAG also establishes new SOTA performance across all evaluation metrics, demonstrating excellent transferability and robustness. These results confirm that HKRAG effectively captures query-relevant holistic knowledge from documents, substantially enhancing retrieval quality. Even when compared with fine-tuned

vision–language models such as DSE, VisRAG-Ret, and VDocRAG, HKRAG consistently delivers superior performance. This advantage primarily stems from our efficient fine-tuning strategy, which enables precise localization of both salient knowledge and fine-grained knowledge.

4.2. Retrieval-Augmented Generation Results

As shown in Table 3, HKRAG-Generator consistently outperforms all competing methods across the four benchmarks. Under the All setting, it delivers clear performance improvements over VDocRAG—raising accuracy on ChartQA by 6.7%, on SlideVQA by 3.5%, on InfoVQA by 3.1%, and on DUDE by 6.4%. These gains stem from the complementary strengths of HKRAG-Retriever and HKRAG-Generator, which jointly enhance both document selection and holistic reasoning over visually rich con-

Method	ChartQA		InfoVQA	
	Single	All	Single	All
Baseline	50.7	44.7	31.5*	29.6*
HKRAG w/o Gen	51.3	49.3	31.9*	31.2*
HKRAG w/o Ret	57.3	52.7	41.9*	38.7*
HKRAG	60.7	58.0	42.7*	39.6*

Table 4. Ablation study of Retriever (Ret) and Generator (Gen) in HKRAG. The baseline employs Eq. 3 for retriever fine-tuning, then directly inputs the generator.

Method	ChartQA		InfoVQA	
	Single	All	Single	All
Baseline	84.4	76.3	70.4*	53.9*
Ret w/o \mathcal{L}_{SIN}	84.9	77.9	71.3*	55.2*
Ret w/o \mathcal{L}_{DIN}	85.7	79.4	70.7*	54.6*
HKRAG-Ret	87.6	82.1	72.4*	57.8*

Table 5. Ablation study of different components in HKRAG-Ret.

Method	ChartQA		InfoVQA	
	Single	All	Single	All
Baseline	51.3	49.3	31.9*	31.2*
Gen w/o pruner	56.0	54.7	40.4*	35.3*
Gen w/o decoupler	59.0	56.3	40.5*	38.0*
HKRAG-Gen	60.7	58.0	42.7*	39.6*

Table 6. Ablation study of different components in HKRAG-Gen.

tent. Even in the Gold setting, HKRAG-Generator achieves up to 4.3% higher accuracy than VDocGenerator, showing that its benefits are not merely due to improved retrieval but rather from more effective holistic-knowledge reasoning. Overall, the results demonstrate that HKRAG-Generator substantially alleviates the holistic-knowledge gap in open-domain visually rich document understanding, enabling more accurate and dependable answer generation.

4.3. Analysis

Effect of each component in HKRAG. Table 4 reports the ablation results of the hybrid masking-based holistic retriever and the uncertainty-guided agentic generator on ChartQA and InfoVQA. Removing either component results in clear performance drops, demonstrating that the two modules play complementary roles. The bidirectional retriever-tuning alone enhances retrieval accuracy by improving query-document alignment, whereas the generator alone yields a more substantial improvement in answer quality by adaptively selecting and reasoning over the informative documents. When both modules are enabled, HKRAG attains the highest performance across all settings, indicating that holistic retrieval and adaptive reasoning syn-

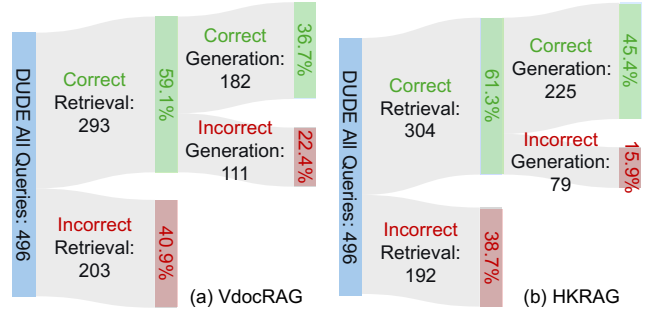


Figure 3. Performance of (a) VDocRAG and (b) HKRAG on DUDE. We present the distribution of queries across two categories: those that retrieved the correct document in the top-3 position (“correct retrieval”), and those that provided the correct answer given the top-3 retrieved documents (“correct generation”).

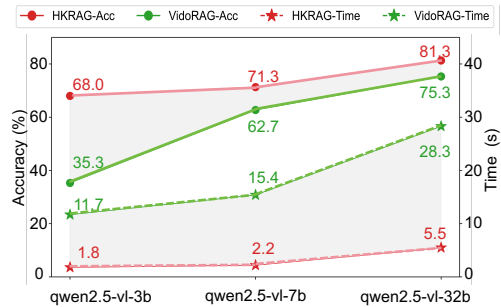


Figure 4. Comparison of VidoRAG [35] and our HKRAG across different sizes within the same series. The shaded area represents the gap between VidoRAG and HKRAG.

ergistically contribute to a more comprehensive understanding of visually rich documents.

How does our retriever gain benefits? Table 5 presents the ablation results for the individual components of the Retriever. Removing either \mathcal{L}_{SIN} or \mathcal{L}_{DIN} leads to clear performance degradation, highlighting their complementary roles. Specifically, \mathcal{L}_{SIN} reinforces fine-print knowledge consistency, while \mathcal{L}_{DIN} strengthens salient knowledge consistency—both essential for reliable retrieval. The full HKRAG-Ret achieves the highest accuracy across all datasets and settings, demonstrating that jointly optimizing these objectives strikes an effective balance between fine-grained alignment and cross-domain generalization.

How does our generator gain benefits? In Table 6, removing the dynamic buffer (Gen w/o pruner), which selects minimal sufficient knowledge documents instead of using fixed-K inputs, causes noticeable performance drops, particularly on InfoVQA, demonstrating its crucial role in efficient knowledge retrieval. Without the decoupler that handles HQP through reasoning disentanglement, performance degrades to 56.3 (ChartQA All) and 38.0 (InfoVQA All),

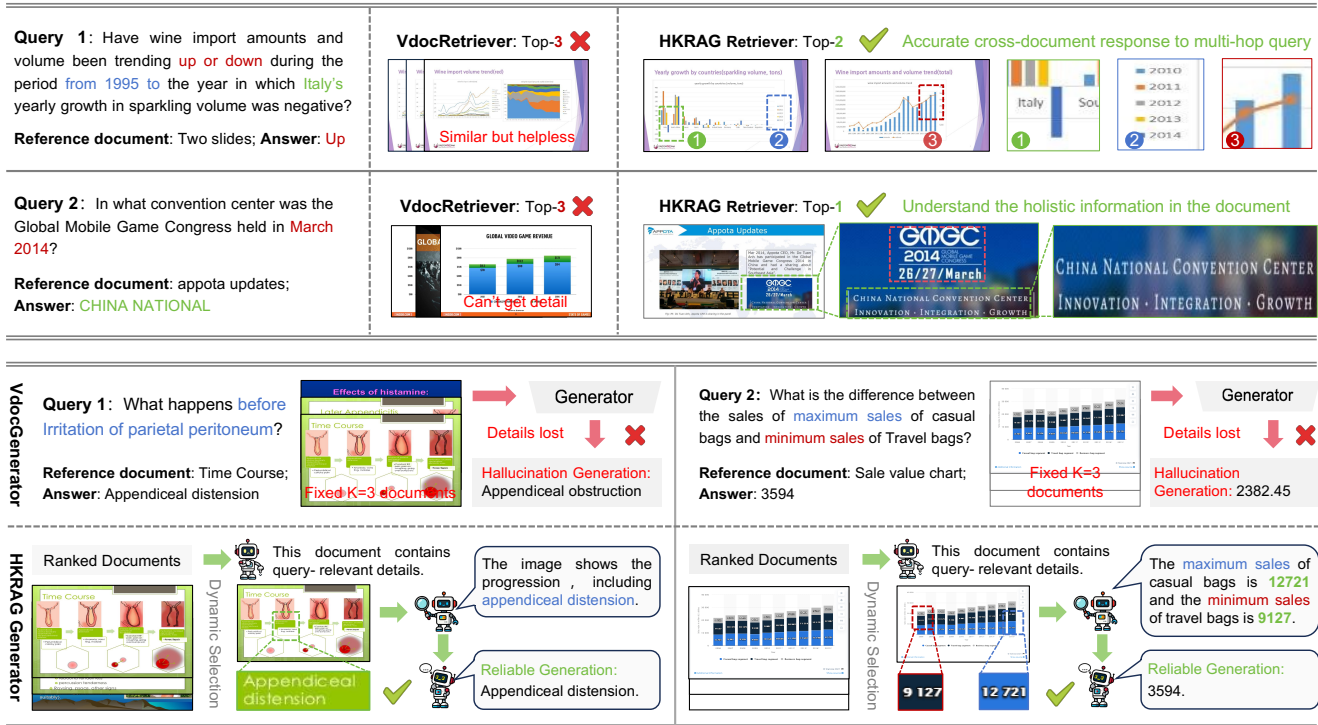


Figure 5. Qualitative results of our HKRAG compared to state-of-the-art VDocRAG [30] on open-domain visually rich documents.

indicating its importance in resolving ambiguous cases. HKRAG-Gen achieves the best results, validating that both components synergistically enhance knowledge selection and reasoning capability.

How accuracy and time efficiency vary under different LVLN? In Figure 4, we demonstrate the accuracy and time efficiency of VidoRAG and HKRAG across different Qianwen 2.5 visual-language models, including 3b, 7b, and 32b. Through comparison, we observe that HKRAG consistently achieves higher accuracy than VidoRAG under identical settings while requiring less computational time. This indicates our generator efficiently and accurately infers answers, owing to our uncertainty-guided reasoning process that extracts holistic information based on uncertainty mining within query-document pairs.

Qualitative results. We present a qualitative comparison with VDocRAG in Figure 5. During the retrieval phase (top), VDocRAG only includes documents semantically similar but irrelevant to Query 1 in its top-3 retrieval results. In contrast, our retriever accurately identifies two documents across the retrieval set that can answer the query, effectively addressing the multi-hop problem. During the generation phase (below), even when VDocRAG accurately retrieves documents containing answers, it generates hallucinations due to the difficulty of precisely inferring the computational relationship between maximum and mini-

imum values from extensive visual information. Notably, our generator efficiently understands logical relationships within instances by dynamically selecting query-relevant documents amidst complex visual information.

5. Conclusion

In this paper, we identify a critical limitation in existing multimodal RAG methods for open-domain DocumentVQA task: their inherent bias toward salient knowledge and consistent oversight of fine-print knowledge, which we term the *inadequate holistic knowledge problem*. To address this, we propose HKRAG, a new multimodal RAG framework that enables holistic retrieval and dynamic integration of both knowledge types. Central to HKRAG are two new components: a hybrid masking-based holistic retriever, which explicitly enhances the model’s sensitivity to both salient and fine-print content through structured feature masking, and an uncertainty-guided agentic generator, which dynamically routes queries based on initial-answer confidence and performs iterative reasoning when needed. Extensive experiments on multiple DocumentVQA benchmarks, including zero-shot (ChartQA, SlideVQA) and supervised (InfoVQA, DUDE) settings, demonstrate that HKRAG consistently outperforms the compared baselines, confirming its robustness and generalizability in achieving truly holistic document understanding.

References

- [1] Marah Abidin, Jyoti Aneja, Hany Awadalla, Ahmed Awadallah, Ammar Ahmad Awan, Nguyen Bach, Amit Bahree, and et al. Arash Bakhtiari. Phi-3 technical report: A highly capable language model locally on your phone. *arXiv preprint arXiv: 2404.14219*, 2024. 5, 6
- [2] Florin Cuconasu, Giovanni Trappolini, Federico Siciliano, Simone Filice, Cesare Campagnano, Yoelle Maarek, Nicola Tonello, and Fabrizio Silvestri. The power of noise: Redefining retrieval for rag systems. In *Proceedings of the 47th International ACM SIGIR Conference on Research and Development in Information Retrieval*, pages 719–729, 2024. 2
- [3] Tri Dao, Dan Fu, Stefano Ermon, Atri Rudra, and Christopher Ré. Flashattention: Fast and memory-efficient exact attention with io-awareness. *NeurIPS*, 35:16344–16359, 2022. 5
- [4] Jacob Devlin, Ming-Wei Chang, Kenton Lee, and Kristina Toutanova. BERT: pre-training of deep bidirectional transformers for language understanding. In *NAACL-HLT*, pages 4171–4186, 2019. 6
- [5] Guanting Dong, Jiajie Jin, Xiaoxi Li, Yutao Zhu, Zhicheng Dou, and Ji-Rong Wen. Rag-critic: Leveraging automated critic-guided agentic workflow for retrieval augmented generation. In *ACL*, pages 3551–3578, 2025. 1, 2
- [6] Tianyu Fan, Jingyuan Wang, Xubin Ren, and Chao Huang. Minirag: Towards extremely simple retrieval-augmented generation. *arXiv preprint arXiv:2501.06713*, 2025.
- [7] Wenqi Fan, Yajuan Ding, Liangbo Ning, Shijie Wang, Hengyun Li, Dawei Yin, Tat-Seng Chua, and Qing Li. A survey on rag meeting llms: Towards retrieval-augmented large language models. In *SIGKDD*, pages 6491–6501, 2024. 1, 2
- [8] Manuel Faysse, Hugues Sibille, Tony Wu, Bilel Omrani, Gautier Viaud, CELINE HUDELLOT, and Pierre Colombo. Colpali: Efficient document retrieval with vision language models. In *ICLR*, 2024. 1, 2, 5
- [9] Zirui Guo, Lianghao Xia, Yanhua Yu, Tu Ao, and Chao Huang. Lightrag: Simple and fast retrieval-augmented generation. *arXiv preprint arXiv:2410.05779*, 2024. 2
- [10] Edward J Hu, Yelong Shen, Phillip Wallis, Zeyuan Allen-Zhu, Yuanzhi Li, Shean Wang, Lu Wang, Weizhu Chen, et al. Lora: Low-rank adaptation of large language models. *ICLR*, 1(2):3, 2022. 5
- [11] Gautier Izacard, Mathilde Caron, Lucas Hosseini, Sebastian Riedel, Piotr Bojanowski, Armand Joulin, and Edouard Grave. Unsupervised dense information retrieval with contrastive learning. *Trans. Mach. Learn. Res.*, 2022, 2022. 2, 5, 6
- [12] Albert Q. Jiang, Alexandre Sablayrolles, Arthur Mensch, Chris Bamford, Devendra Singh Chaplot, Diego de las Casas, Florian Bressand, Gianna Lengyel, Guillaume Lample, Lucile Saulnier, Léo Renard Lavaud, Marie-Anne Lachaux, Pierre Stock, Teven Le Scao, Thibaut Lavril, Thomas Wang, Timothée Lacroix, and William El Sayed. Mistral 7b. *arXiv preprint arXiv: 2310.06825*, 2023. 6
- [13] Ehsan Kamaloo, Nandan Thakur, Carlos Lassance, Xueguang Ma, Jheng-Hong Yang, and Jimmy Lin. Re-sources for brewing beer: Reproducible reference models and statistical analyses. In *SIGIR*, pages 1431–1440, 2024. 5
- [14] Sunjun Kweon, Yeonsu Kwon, Seonhee Cho, Yohan Jo, and Edward Choi. Open-wikitable: Dataset for open domain question answering with complex reasoning over table. *arXiv preprint arXiv:2305.07288*, 2023. 1, 2, 5
- [15] Chankyu Lee, Rajarshi Roy, Mengyao Xu, Jonathan Raiman, Mohammad Shoeybi, Bryan Catanzaro, and Wei Ping. Nv-embed: Improved techniques for training llms as generalist embedding models. In *ICLR*, 2025. 2, 5, 6
- [16] Zehan Li, Xin Zhang, Yanzhao Zhang, Dingkun Long, Pengjun Xie, and Meishan Zhang. Towards general text embeddings with multi-stage contrastive learning. *arXiv preprint arXiv: 2308.03281*, 2023. 2, 5, 6
- [17] Ilya Loshchilov and Frank Hutter. Decoupled weight decay regularization. *arXiv preprint arXiv:1711.05101*, 2017. 5
- [18] Yongdong Luo, Xiawu Zheng, Xiao Yang, Guilin Li, Haojia Lin, Jinfa Huang, Jiayi Ji, Fei Chao, Jiebo Luo, and Rongrong Ji. Video-rag: Visually-aligned retrieval-augmented long video comprehension. *arXiv preprint arXiv:2411.13093*, 2024. 2
- [19] Xueguang Ma, Sheng-Chieh Lin, Minghan Li, Wenhua Chen, and Jimmy Lin. Unifying multimodal retrieval via document screenshot embedding. In *EMNLP*, pages 6492–6505, 2024. 1, 2, 5, 6
- [20] Ahmed Masry, Xuan Long Do, Jia Qing Tan, Shafiq Joty, and Enamul Hoque. Chartqa: A benchmark for question answering about charts with visual and logical reasoning. In *ACL Findings*, pages 2263–2279, 2022. 1, 2, 5
- [21] Minesh Mathew, Dimosthenis Karatzas, and CV Jawahar. Docvqa: A dataset for vqa on document images. In *WACV*, pages 2200–2209, 2021. 5
- [22] Minesh Mathew, Viraj Bagal, Rubèn Tito, Dimosthenis Karatzas, Ernest Valveny, and CV Jawahar. Infographicvqa. In *WACV*, pages 1697–1706, 2022. 5
- [23] Marjorie A Oettinger, David G Schatz, Carolyn Gorka, and David Baltimore. Rag-1 and rag-2, adjacent genes that synergistically activate v (d) j recombination. *Science*, 248(4962): 1517–1523, 1990. 2
- [24] Aaron van den Oord, Yazhe Li, and Oriol Vinyals. Representation learning with contrastive predictive coding. *arXiv preprint arXiv:1807.03748*, 2018. 4
- [25] Alec Radford, Jong Wook Kim, Chris Hallacy, Aditya Ramesh, Gabriel Goh, Sandhini Agarwal, Girish Sastry, Amanda Askell, Pamela Mishkin, Jack Clark, Gretchen Krueger, and Ilya Sutskever. Learning transferable visual models from natural language supervision. In *ICML*, pages 8748–8763, 2021. 5, 6
- [26] Xubin Ren, Lingrui Xu, Long Xia, Shuaiqiang Wang, Dawei Yin, and Chao Huang. Videorag: Retrieval-augmented generation with extreme long-context videos. *arXiv preprint arXiv:2502.01549*, 2025. 2
- [27] Stephen E. Robertson and Hugo Zaragoza. The probabilistic relevance framework: BM25 and beyond. *Found. Trends Inf. Retr.*, 3(4):333–389, 2009. 2, 5, 6
- [28] Ryota Tanaka, Kyosuke Nishida, and Sen Yoshida. Visualmrc: Machine reading comprehension on document im-

- ages. In *Proceedings of the AAAI Conference on Artificial Intelligence*, pages 13878–13888, 2021. [1](#), [2](#), [5](#)
- [29] Ryota Tanaka, Kyosuke Nishida, Kosuke Nishida, Taku Hasegawa, Itsumi Saito, and Kuniko Saito. Slidevqa: A dataset for document visual question answering on multiple images. In *Proceedings of the AAAI Conference on Artificial Intelligence*, pages 13636–13645, 2023. [1](#), [2](#), [5](#)
- [30] Ryota Tanaka, Taichi Iki, Taku Hasegawa, Kyosuke Nishida, Kuniko Saito, and Jun Suzuki. Vdocrag: Retrieval-augmented generation over visually-rich documents. In *CVPR*, pages 24827–24837, 2025. [2](#), [5](#), [6](#), [8](#)
- [31] Yubao Tang, Ruqing Zhang, Jiafeng Guo, Maarten de Rijke, Yixing Fan, and Xueqi Cheng. Boosting retrieval-augmented generation with generation-augmented retrieval: A co-training approach. In *SIGIR*, pages 2441–2451, 2025. [1](#), [2](#)
- [32] Jordy Van Landeghem, Rubèn Tito, Łukasz Borchmann, Michał Pietruszka, Paweł Joziak, Rafał Powalski, Dawid Jurkiewicz, Mickaël Coustaty, Bertrand Anckaert, Ernest Valveny, et al. Document understanding dataset and evaluation (dude). In *ICCV*, pages 19528–19540, 2023. [1](#), [2](#), [5](#)
- [33] Liang Wang, Nan Yang, Xiaolong Huang, Binxing Jiao, Linjun Yang, Daxin Jiang, Rangan Majumder, and Furu Wei. Text embeddings by weakly-supervised contrastive pre-training. *arXiv preprint arXiv: 2212.03533*, 2024. [2](#), [5](#), [6](#)
- [34] Liang Wang, Nan Yang, Xiaolong Huang, Linjun Yang, Rangan Majumder, and Furu Wei. Improving text embeddings with large language models. In *ACL*, pages 11897–11916, 2024. [2](#), [5](#), [6](#)
- [35] Qiuchen Wang, Ruixue Ding, Zehui Chen, Weiqi Wu, Shihang Wang, Pengjun Xie, and Feng Zhao. Vidorag: Visual document retrieval-augmented generation via dynamic iterative reasoning agents. *EMNLP*, 2025. [5](#), [7](#)
- [36] Peng Xu, Wenqi Shao, Kaipeng Zhang, Peng Gao, Shuo Liu, Meng Lei, Fanqing Meng, Siyuan Huang, Yu Qiao, and Ping Luo. Lvlm-ehub: A comprehensive evaluation benchmark for large vision-language models. *IEEE Transactions on Pattern Analysis and Machine Intelligence*, 2024. [2](#)
- [37] Xiao Yang, Kai Sun, Hao Xin, Yushi Sun, Nikita Bhalla, Xiangsen Chen, Sajal Choudhary, Rongze D Gui, Ziran W Jiang, Ziyu Jiang, et al. Crag-comprehensive rag benchmark. *NeurIPS*, 37:10470–10490, 2024. [2](#)
- [38] Yuan Yao, Tianyu Yu, Ao Zhang, Chongyi Wang, Junbo Cui, Hongji Zhu, Tianchi Cai, Haoyu Li, Weilin Zhao, Zhihui He, Qianyu Chen, Huarong Zhou, Zhensheng Zou, Haoye Zhang, Shengding Hu, Zhi Zheng, Jie Zhou, Jie Cai, Xu Han, Guoyang Zeng, Dahai Li, Zhiyuan Liu, and Maosong Sun. Minicpm-v: A GPT-4V level MLLM on your phone. *arXiv preprint arXiv: 2408.01800*, 2024. [6](#)
- [39] Shi Yu, Chaoyue Tang, Bokai Xu, Junbo Cui, Junhao Ran, Yukun Yan, Zhenghao Liu, Shuo Wang, Xu Han, Zhiyuan Liu, et al. Visrag: Vision-based retrieval-augmented generation on multi-modality documents. In *ICLR*, 2025. [1](#), [2](#), [6](#)